

PII: S0017-9310(97)00211-1

# Similarity of heat radiation from turbulent buoyant jets

A. I. BRIL, V. P. KABASHNIKOV, N. V. KUZMINA and V. M. POPOV

Institute of Physics of the Belarusian Academy of Sciences, Minsk, 220072, Belarus

(Received 16 May 1996)

**Abstract**—The thermal radiation similarity of buoyant turbulent jets is studied. The principal condition for the radiation similarity is the similarity of the temperature and the concentration fields in the near-nozzle region because the main part of radiation is generated by this most heated section of the jet. The  $k$ - $\epsilon$ - $T'^2$  turbulent viscosity model is used to study numerically the gas dynamic similarity in the near-nozzle zone. It is shown that the excess temperature and concentration fields of different jets can be described by a universal function of the dimensionless coordinates that are longitudinal and transverse coordinates normalized with respect to the special longitudinal and transverse scales. It is found, as a result of the gas dynamic similarity, that the dimensionless spectral intensity (normalized with respect to the production of spectral radiance at the edge of the nozzle and the nozzle area) is described by a universal function which is the same for a wide class of jets and which depends on the exit parameters, radiation frequency and on the steepness of the temperature dependence of the absorption coefficient. The results obtained are generalized for the case of molecular gas radiation in finite spectral intervals containing many spectral lines. A simple and effective method for jet radiation prediction, which does not require a detailed information about the jet gas dynamic structure, is developed. © 1998 Published by Elsevier Science Ltd.

## 1. INTRODUCTION

In this work the results of the investigation of thermal radiation for turbulent convective vertical jets are presented. Our purpose was to generalise the relationships of an optical similarity, established previously experimentally and theoretically, and to extend them to buoyant jets [1, 2]. The phenomenon of an optical similarity consists in a possibility to introduce universal functions that would describe thermal radiation for a wide class of jets with various initial parameters.

Just as in refs. [1, 2], in the present work only the case of optically thin radiation is considered. In other words, it is assumed that the path length of a quantum considerably exceeds the characteristic size of flow. In typical jets of hydrocarbon fuel combustion products the radiation is usually optically thin for minor impurities (soot, oxides of nitrogen, sulphur and so on). But in the centres of bands of basic combustion products such as water vapour and carbon dioxide, the jets, as a rule, are not optically thin. However, at large observation distances the  $H_2O$  and  $CO_2$  radiation, filtered by the atmosphere, is concentrated mainly at the frequencies, where a radiating volume is optically thin. This circumstance greatly increases a number of situations when optically thin radiation is valid.

A primary condition for an optical similarity is the gas dynamic similarity of flows. The similarity of gas dynamic characteristics in the far field of jet flows is the well-known fact. However, the main portion of thermal radiation is generated by the most heated

near-nozzle section of a jet (near field). In the near field the flow depends strongly on a number of uncertain or poorly measured initial parameters, in particular, on the initial level of turbulence kinetic energy. Nevertheless it was shown that for the near field of non-buoyant jets some universal relationships for the gas dynamic parameters are approximately valid if we use special longitudinal scale  $X_T$ .

It was shown previously [1, 2] on the basis of experimental and numerical investigations, that distributions of temperature and concentration for non-buoyant round jets in a wide range of initial flow parameters can approximately be reduced to unified relationships:

$$\frac{T(x, r) - T_\infty}{T_0 - T_\infty} = \frac{C(x, r) - C_\infty}{C_0 - C_\infty} = f(\xi, \eta), \quad R_T = R_T(\xi) \quad (1)$$

where  $x$  and  $r$  are the cylindrical coordinates,  $\xi = x/X_T$ ,  $\eta = r/R_T$ ,  $X_T$  is equal to the value of  $x$  at which  $\Delta T_c = 0.75\Delta T_0$ , and  $R_T$  is equal to the value of  $r$  at which the excess temperature is half its axial value. The longitudinal scale  $X_T$  depends on the initial parameters of the flow ( $\rho_0/\rho_\infty$ , initial level of turbulent kinetic energy  $k_0$ , etc.).

There are no indications in the literature (within the knowledge of the authors) of a gas dynamic similarity in the near field of buoyant jets. Therefore, in the next section we attempt to establish such properties on the basis of a numerical model checked out on the known experimental data.

## NOMENCLATURE

$B$	Planck function	$V$	mean velocity component in radial direction
$c$	speed of light	$v$	fluctuating velocity component in radial direction
$C_n$	concentration of $n$ th gaseous component	$\overline{vT'}$	turbulent heat flux, radial component
$C^*$	$F^{1/2}(\rho_c - \rho_\infty)/(\rho_0 - \rho_\infty)$	$x$	axial coordinate
$D$	jet exit diameter	$X_T$	axial scale of jet temperature
$d$	averaged distance between spectral lines	$X^*$	$= F^{-1/2}(x/D)$
$f(\xi, \eta)$	universal function describing excess temperature and concentration	$y$	distance between line of viewing and jet axis.
$F$	Froude number	Greek symbols	
$g$	acceleration of gravity	$\gamma$	spectral line half-width
$h$	Planck's constant	$\Delta T$	$= T - T_\infty$
$I$	spectral radiance	$\Delta\nu$	spectral frequency range
$k$	turbulent kinetic energy, Boltzmann's constant	$\varepsilon$	dissipation rate of turbulent kinetic energy
$k_{STP}$	absorption coefficient at standard temperature and pressure	$\eta$	radial dimensionless coordinate
$r$	radial coordinate	$\lambda$	radiation wavelength
$R_0$	$D/2$	$\nu$	radiation frequency
$R_T$	radial scale of jet temperature	$\rho$	mean density
$S$	spectral intensity	$\tau$	transmittance of the atmosphere
$T$	mean temperature	$\xi$	axial dimensionless coordinate.
$U$	mean velocity component in axial direction	Subscripts	
$u$	fluctuating velocity component in axial direction	0	exit condition
$U^*$	$= F^{1/2}(U_c/U_0)$	$\infty$	ambient condition
$\overline{uv}$	turbulent shear stress, axial component	$c$	centreline value
$\overline{uT'}$	turbulent heat flux, axial component	$m$	corresponds to $m$ th spectral group
		$n$	corresponds to $n$ th molecular component.

## 2. NUMERICAL SIMULATION OF THE GAS DYNAMIC STRUCTURE OF A TURBULENT BUOYANT JET

The governing equations for velocity and temperature distributions in a vertical buoyant axially symmetric jet can be written as:

$$\frac{\partial(\rho U)}{\partial x} + \frac{1}{r} \frac{\partial}{\partial r}(r \rho V) = 0, \quad (2)$$

$$\rho U \frac{\partial U}{\partial x} + \rho V \frac{\partial U}{\partial r} = \frac{1}{r} \frac{\partial}{\partial r}(-r \rho \overline{uv}) + \rho \frac{g}{T_\infty}(T - T_\infty), \quad (3)$$

$$\rho U \frac{\partial T}{\partial x} + \rho V \frac{\partial T}{\partial r} = \frac{1}{r} \frac{\partial}{\partial r}(-r \rho \overline{vT'}), \quad (4)$$

where  $U$  and  $V$  are the mean velocity components in axial and normal directions,  $T$  and  $\rho$  are the mean jet temperature density.

To calculate the components of turbulent stresses  $\overline{uv}$  and heat fluxes  $\overline{vT'}$ , occurring in eqns (3) and (4), we used the  $k$ - $\varepsilon$ - $T'^2$  model [3, 4], within the framework of which the parameters of the turbulence field  $k$  (turbulent kinetic energy),  $\varepsilon$  (dissipation rate of  $k$ ) and  $T'^2$  (mean-square fluctuations of temperature) are determined by the equations

$$\rho U \frac{\partial k}{\partial x} + \rho V \frac{\partial k}{\partial r} = \frac{1}{r} \frac{\partial}{\partial r} \left( r \rho c_k \frac{\overline{kv^2}}{\varepsilon} \frac{\partial k}{\partial r} \right) - \frac{\overline{uv}}{\rho} \frac{\partial U}{\partial r} + \rho \frac{g \overline{uT'}}{T_\infty} - \rho \varepsilon, \quad (5)$$

$$\rho U \frac{\partial \varepsilon}{\partial x} + \rho V \frac{\partial \varepsilon}{\partial r} = \frac{1}{r} \frac{\partial}{\partial r} \left( r \rho c_\varepsilon \frac{\overline{kv^2}}{\varepsilon} \frac{\partial \varepsilon}{\partial r} \right) + c_{\varepsilon 1} \rho \frac{\varepsilon}{k} \left( -\frac{\overline{uv}}{\rho} \frac{\partial U}{\partial r} + \frac{g \overline{uT'}}{T_\infty} \right) - c_{\varepsilon 2} \rho \frac{\varepsilon^2}{k}, \quad (6)$$

$$\rho U \frac{\partial \overline{T'^2}}{\partial x} + \rho V \frac{\partial \overline{T'^2}}{\partial r} = \frac{1}{r} \frac{\partial}{\partial r} \left( r \rho c_T \frac{k^2}{\varepsilon} \frac{\partial \overline{T'^2}}{\partial r} \right) - 2\rho \overline{vT'} \frac{\partial T}{\partial r} - c_{T1} \rho \frac{\varepsilon \overline{T'^2}}{k} \quad (7)$$

Following ref. [3], the components of turbulent stresses and heat fluxes will be calculated using the following algebraic relations

$$-\overline{uv} = \frac{1-c_0}{c_1} \frac{\overline{v^2}}{k} \left[ 1 + \frac{kg}{c_h \varepsilon T_\infty} \frac{\partial T}{\partial r} \frac{\partial U}{\partial r} \right] \frac{k^2}{\varepsilon} \frac{\partial U}{\partial r} \quad (8)$$

$$\overline{v^2} = c_2 k, \quad (9)$$

$$-\overline{vT'} = \frac{1}{c_h} \frac{\overline{v^2}}{k} \frac{k^2}{\varepsilon} \frac{\partial T}{\partial r} \quad (10)$$

$$-\overline{uT'} = \frac{k}{c_h \varepsilon} \left[ -\overline{uv} \frac{\partial T}{\partial r} - \overline{vT'} (1-c_h) \frac{\partial U}{\partial r} + \frac{g(1-c_{h1})}{T_\infty} \overline{T'^2} \right] \quad (11)$$

The system of eqns (2)–(11) includes 11 empirical constants. We adopted the same constant values as in ref. [3]:  $c_0 = 0.55$ ;  $c_1 = 2.2$ ;  $c_2 = 0.23$ ;  $c_\varepsilon = 0.15$ ;  $c_{\varepsilon 1} = 1.43$ ;  $c_{\varepsilon 2} = 1.92$ ;  $c_k = 0.225$ ;  $c_T = 0.13$ ;  $c_{T1} = 1.25$ ;  $c_h = 3.2$ ;  $c_{h1} = 0.5$ . We also adopted the correction function used in ref. [3]:

$$Q = \left| \frac{\Delta r_c}{2U_c} \left( \frac{dU_c}{dx} - \left| \frac{dU_c}{dx} \right| \right) \right|^{0.2}$$

where  $U_c$  is the axial velocity,  $\Delta r_c$  is the distance from the jet centreline to a point, where  $U = 0.5U_c$ . The right-hand side of equality (8) is multiplied by  $(1 - 0.465Q)$ , and  $c_{\varepsilon 2}$  is multiplied by  $(1 - 0.035Q)$ . The uniform (stepwise) profiles of velocity, temperature and concentration, as well as the fluctuation parameters  $k$ ,  $\varepsilon$  and  $\overline{T'^2}$  were used as initial conditions (at  $x = 0$ ).

The results of comparison of the calculated and measured distributions of axial temperature in the jet near field for three values of Froude number  $F = \rho_0 U_0 / gD(\rho_\infty - \rho_0)$  are presented in Fig. 1. Experimental data obtained by Pryputniewicz are used [3]. The calculations were carried out using Boussinesq approximation, within which the dependence on gas density is preserved only in the gravitational term of eqn (3) (since in ref. [3] only initial values of  $F$  are indicated). The following initial values of the parameters were chosen:  $k_0 = 0.01U_0^2$ ,  $\varepsilon_0 = 0.004U_0^3/D$  and  $\overline{T_0'^2} = 0.01(T_0 - T_\infty)$ . (Hereafter, if the values of  $k_0$ ,  $\varepsilon_0$  or  $\overline{T_0'^2}$  are not indicated, it is understood that the above-mentioned values are used.) Calculated axial profiles  $C^* = F^{1/2}(\rho_c - \rho_\infty)/(\rho_0 - \rho_\infty)$  and  $U^* = F^{1/2}(U_c/U_0)$  as functions of the normalised coordinate  $X^* = F^{1/2}(x/D)$  in a convective flow region (far

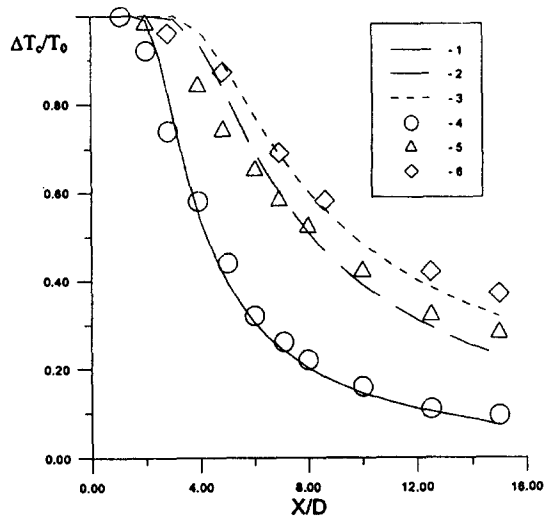


Fig. 1. Comparison of the predicted and measured axial profiles of the excess temperature. 1–3, predictions; 4–6, experiment [3]. 1, 4— $F = 1$ ; 2, 5— $F = 25$ ; 3, 6— $F = 625$ .

field) are presented in Fig. 2. It can be seen that the model used satisfactorily describes the known asymptotic relationships [4, 5]. (These calculations were also carried out using Boussinesq approximation, so the ratio  $\rho_0/\rho_\infty$  in asymptotic relationships was assumed to be equal to 1.) The comparisons presented, that virtually reproduce separate calculations, and comparisons from [3, 4], show that the given model adequately describes the distributions of flow parameter in the near and far fields of turbulent buoyant jets and can be used for numerical investigations of gas dynamic similarity criteria in the near field of a jet with account of thermogravity effects.

### 3. GAS DYNAMIC SIMILARITY CRITERIA IN THE NEAR FIELD OF A BUOYANT JET

Following [1, 2], we chose as a longitudinal scale of flow, a value of an axial coordinate, at which an excess axial temperature decreases to 0.75 of its initial value. On the basis of numerical investigations carried out using the above-described model we established the following regularities.

(A) For vertical buoyant jets the above-defined longitudinal scale  $X_T$  depends strongly on the Froude number. Nevertheless, the normalization of the longitudinal coordinate using  $X_T$  allows one to reduce the axial profiles of the excess temperature approximately to a universal function of  $\xi$  for a wide range of change in the Froude number  $F$  (Fig. 3(a)). However, as can be seen from Fig. 3(b), there is no universal dependence of  $R_T$  on  $\xi$ , i.e.,  $R_T$  depends not only on  $\xi$ , but also on  $F$ . The non-monotonic dependence of  $R_T$  on  $\xi$  follows from the condition of buoyancy conservation in the near field of jet: the jet thermal transverse size decreases as with an increase in the jet velocity due to the Archimedean force. The results

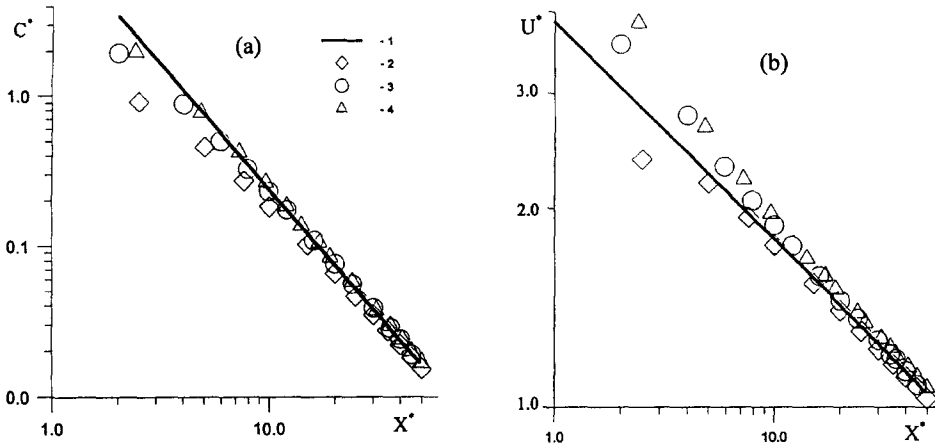


Fig. 2. Asymptotic behaviour of the axial distributions of density (a) and velocity (b) in a buoyant vertical jet. 1, (a):  $C^* = 11X^{*-5/3}$ ; (b):  $U^* = 3.9X^{*-1/3}$ . 2,  $F = 1$ ; 3,  $F = 6.3$ ; 4,  $F = 39.3$ .

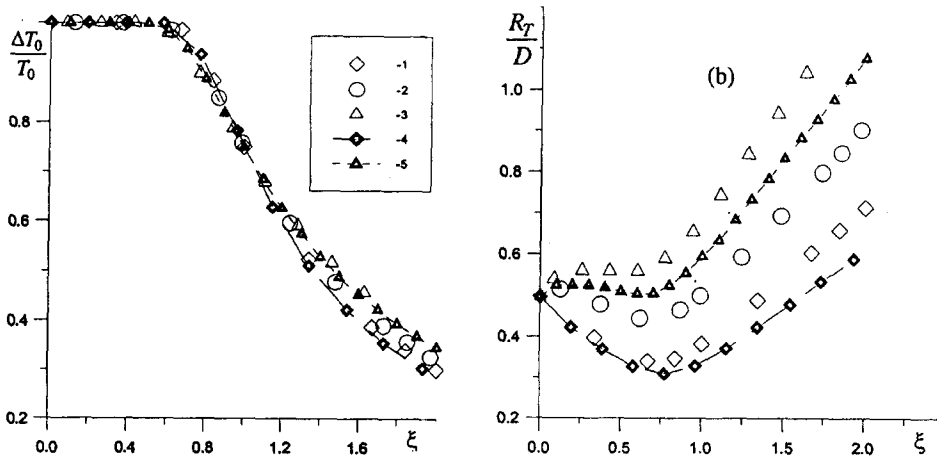


Fig. 3. Dependence of the excess temperature (a) and radial thermal scale (b) on the axial coordinate for various values of the Froude number. 1, 4,  $F = 1$ ; 2,  $F = 5$ ; 3, 5,  $F = 50$ . 1-3 correspond to calculation with the use of the Boussinesq approximation, and 4 and 5 to calculation without using this approximation.

calculated both with and without the use of an Boussinesq approximation are presented in Fig. 3. It can be seen that the  $T_c$  and  $R_T$  profiles depend weakly on the chosen approach. It was considered as a sufficient reason for using the Boussinesq approximation in further numerical investigations.

(B) The radial profiles of the excess temperature and concentration are described rather accurately by universal relationships not only for a wide range of Froude numbers (Fig. 4), but also, as will be discussed below, for various levels of initial turbulence. The weak dependence of  $f(\xi, \eta)$  on  $F$  means that for buoyant jets it is possible to use universal profiles obtained experimentally for non-buoyant jets that were investigated rather thoroughly.

(C) The construction of universal longitudinal profiles of  $T$  and  $C$  for jets with different initial levels of turbulence is most problematic. The longitudinal scale  $X_T$  we selected depends strongly on  $k_0$  and  $\epsilon_0$ , but the

influence of the initial level of turbulence is "forgotten" by the flow downstream from the jet exit plane and the use of  $X_T$  for constructing unified correlations for the far jet field is obviously inapplicable. Nevertheless, for non-buoyant jets the experimental and numerical investigations showed that the introduction of  $X_T(k_0, \epsilon_0)$  for the areas near the jet exit ( $\xi < 2$ ) allows one to use universal profiles of type (1), with an error not exceeding 10–15% for a rather wide range of  $k_0$  and  $\epsilon_0$ . The longitudinal profiles of  $\Delta T_c(\xi)/\Delta T_0$  and  $R_T(\xi)$  for non-buoyant jets, corresponding to three initial values of the turbulent kinetic energy varied by using replaceable conic nozzles are presented in Fig. 4 [6]. Calculations for non-buoyant jets were carried out using the  $k-\epsilon$  model proposed by Launder [7]. The values of  $k_0$  and  $\epsilon_0$  used for calculations were selected on the basis of the best agreement between experimental and calculated profiles of temperature and concentration.

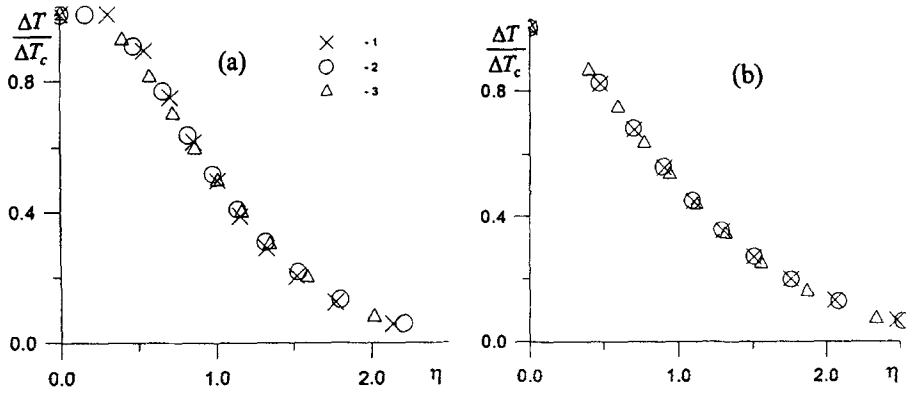


Fig. 4. Radial profiles of the excess temperature in dimensionless coordinates. (a):  $\xi = 0.5$ ; (b):  $\xi = 1.5$ ,  $F = 1; 2, F = 5; 3, F = 50$ .

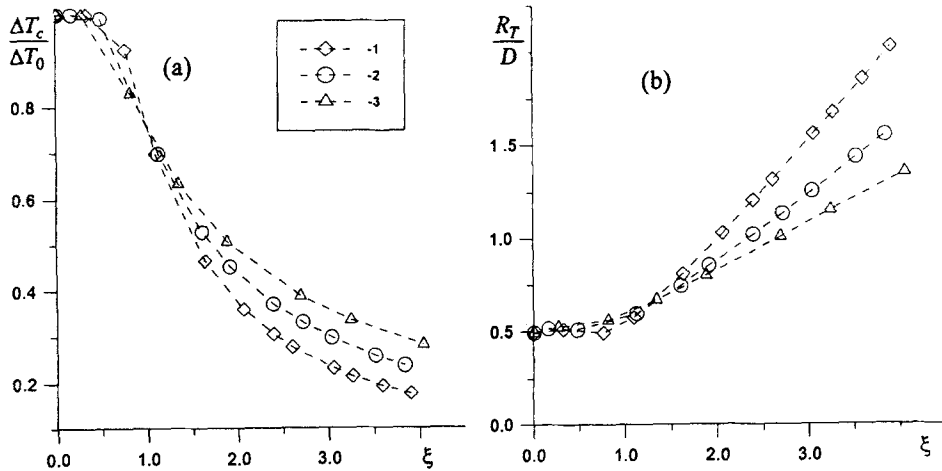


Fig. 5. Dependence of the excess temperature (a) and radial thermal scale (b) on the dimensionless axial coordinate on a non-buoyant jet for various initial levels of turbulence. 1,  $k_0 = 0.0022U_0^2$ ;  $\varepsilon_0 = 0.0003U_0^3/D$ ; 2, 0.01; 0.0014; 3, 0.04; 0.0074.

The corresponding results for the near field of buoyant jets are presented in Fig. 5 (the calculations were carried out for the same values of  $k_0$  and  $\varepsilon_0$  as in Fig. 4). As in the case of non-buoyant jets, the axial profiles of excess temperature can be approximated by a universal function of  $\xi$ . The radial profiles of excess temperature can also be considered as similar (these profiles are practically not distinguished from those presented in Fig. 4). However, the  $R_T$  profiles are close to each other only at low and moderate levels of initial turbulence (the  $k_0$  values are equal to  $0.0022U_0^2$  and  $0.01U_0^2$ ), but for  $k_0 = 0.04U_0^2$  the  $R_T$  dependence on  $\xi$  becomes monotonic (the minimum is vanished). Such behaviour is due to the fact that at high initial levels of turbulence the unmixed flow core becomes very short so that the jet has no time to accelerate significantly and there is no flow region where  $R_T$  decreases. The results obtained are considered as preliminary because we have no experimental data for buoyant jets that agree with or contradict the results

of numerical investigations. At the present stage of our study we consider the flows with not very large variations of the initial values of  $k_0$  and  $\varepsilon_0$  for which only longitudinal scale  $X_T$ , but not radial scale  $R_T$ , depends on  $k_0$  and  $\varepsilon_0$ . This means that we can introduce the following characteristic scales (longitudinal and radial) for convective vertical jets

$$X_T = X_T(k_0, \varepsilon_0, F), \quad R_T = R_T(\xi, F), \quad (12)$$

which allow us to generalise the approximate relations (1), describing excess temperature and concentration profiles for buoyant vertical jets.

#### 4. THERMAL RADIATION SIMILARITY OF BUOYANT JETS

We consider thermal monochromatic radiation of a jet with one optically active component and assume that the background radiation is the Planck radiation

with the temperature  $T_\infty$ . Within an optically thin approximation, the radiance contrast of the jet in the direction perpendicular to the jet symmetry axis is determined by the expression

$$I(x, y) = 2\tau \int_y^\infty \frac{r dr}{\sqrt{r^2 - y^2}} [B(T) - B(T_\infty)] \\ k_{\text{STP}}(T) \frac{300}{T} C(r, x), \quad (13)$$

where  $y$  is the distance between the line of sight and the jet axis;  $B$  is the Planck function;  $k_{\text{STP}}$  is the gas absorption coefficient reduced to the standard temperature and pressure;  $\tau$  is the atmosphere transmittance. Here, the indices that indicate the radiation frequency are omitted for simplicity. Note that volumetric concentration should be used in expression (13), whereas similarity relations (1) are satisfied for mass concentration. However, eqns (1) are also valid for volumetric concentrations if an average molecular weight of a flowing-out gas mixture is approximately equal to the ambient one. This usually holds for exhaust jets with a large amount of excess air.

Along with gas dynamic similarity the unified temperature dependence of the absorption coefficient at all the frequencies and for all the radiative components is needed for optical similarity. This dependence can be presented by the following approximate expression that is valid over a wide range of temperatures:

$$\frac{300}{T} k_{\text{STP}} = \theta \exp\left(-\frac{a}{T}\right), \quad (14)$$

where  $a$  and  $\theta$  are the parameters that depend on frequency and on the type of radiative component. The radiation intensity of the near outlet jet section with the length  $x$  is given by the expression

$$S(x) = 2 \int_0^x dx \int_0^\infty dy I(x, y). \quad (15)$$

If the values  $R_T$  and  $X_T$  are normalized with respect to the nozzle radius  $R_0$  the following relations take place in the Wien spectra region

$$S(x) = I_0 X_T (k_0, \varepsilon_0, F) R_0 G\left(\xi, F, \frac{a}{T_0}, \frac{h\nu}{T_0}, \frac{\Delta T_0}{T_0}, \frac{\Delta C_0}{C_0}\right), \quad (16)$$

where

$$I_0 = 2R_0 C_0 k_{\text{STP}}(T_0) \frac{300}{T_0} [(B(T_0) - B(T_\infty))] \\ = 2R_0 C_0 q (e^{-b/\kappa T_0} - e^{-b/\kappa T_\infty}) e^{-a/\kappa T_0}, \quad (17)$$

$$G = \left(1 - \frac{\Delta C_0}{C_0}\right) G_0 + \frac{\Delta C_0}{C_0} G_1, \quad (18)$$

$$G_k = \left[ g_k\left(\xi, F, \frac{A}{T_0}, \frac{\Delta T_0}{T_0}\right) - \exp\left(-\frac{b\alpha(1)}{T_0}\right) \cdot g_k\left(\xi, F, \frac{a}{T_0}, \frac{\Delta T_0}{T_0}\right) \right] \\ \cdot \left[ 1 - \exp\left(-\frac{b\alpha(1)}{T_0}\right) \right]^{-1} \quad (k = 0, 1), \quad (19)$$

$$g_k\left(\xi, F, p, \frac{\Delta T_0}{T_0}\right) = \pi \int_0^\xi R_T^2(\xi, F) d\xi \\ \times \int_0^\infty \eta d\eta f^k \exp[-p\alpha(\varphi)] \quad (k = 0, 1), \quad (20)$$

$$\alpha(\varphi) = t\varphi/(1-t\varphi), \quad t = \frac{\Delta T_0}{T_0}, \quad \varphi = 1 - f(\xi, \eta), \quad (21)$$

where  $A = a + b$ ,  $b = hc\nu/k$ ,  $q = 2hc^2\nu^3\theta$ ,  $\nu$  is the radiation frequency expressed in reciprocal centimeters,  $h$  is Planck's constant; here,  $k$  is Boltzmann's constant,  $c$  is the speed of light,  $f(\xi, \eta)$  is defined by eqn (1).

Thus, the jet radiation intensity can be written using two universal functions  $g_0$  and  $g_1$ , each being dependent on four arguments. Considerable simplifications take place, however, in some limiting practically important cases.

(i) If the outlet concentration of the radiating gas greatly exceeds that of the ambient gas ( $C_\infty/C_0 \ll 1$ ), the jet radiation intensity is determined only by the function  $g_1$ .

(ii) If the Planck function at jet temperature significantly exceeds the background radiance ( $b\alpha(1)/T_0 \gg 1$ ), we have

$$G_k = g_k\left(\xi, F, \frac{A}{T_0}, \frac{\Delta T_0}{T_0}\right). \quad (19')$$

(iii) It follows from eqn (20) that the magnitude of  $t\varphi$  can be neglected in the denominator of the expression for  $\alpha(\varphi)$  eqn (21) if the jet temperature is low enough ( $t \ll 1$ ) or if the parameter  $p \gg 1$ . As a result, the number of arguments of the functions  $g_k$  is reduced to three:

$$g_k = g_k(\xi, F, pt). \quad (22)$$

All the three cases mentioned occur simultaneously in the short-wave region of the spectrum in the absence of the radiative component in the ambient air. Then the radiation intensity of the jet can be expressed by

$$G = g_1\left(\xi, F, \frac{A\Delta T_0}{T_0^2}\right). \quad (23)$$

Optical similarity relations established previously

for non-buoyant jets [1, 2] follow from eqns (16)–(21) as a particular case under the condition  $F \rightarrow \infty$ .

Expressions (16)–(23) can be proposed for the development of the optical diagnostic techniques. The radiation intensity of the near nozzle jet section depends on the magnitudes of  $k_0$  and  $\epsilon_0$ . As a rule, they are unknown and, therefore, the optical signal carries uncertain information. But if only  $X_T$  depends strongly on  $k_0$  and  $\epsilon_0$  and the dependence of  $R_T(\xi)$  and  $f(\xi, \eta)$  on these parameters can be neglected, the ratio of spectral intensities for different frequencies does not depend on the initial turbulence level and can be used for estimating of the temperature or the ratio of the concentrations for different components.

**5. THERMAL RADIATION OF MOLECULAR GAS JETS**

The jet radiation averaged over the finite spectral interval  $\Delta\nu \sim 10\text{--}50 \text{ cm}^{-1}$  is often of main interest. In the case of molecular gas emission that interval contains a great quantity of spectral lines. The frequency-averaged radiation is often calculated by using the statistical band model which implies that the frequency averaging can be replaced by the averaging over the positions of spectral lines [8, 9]. We used the three-group method [10], based on the statistical band model, to estimate the frequency-averaged radiation. The AFGL [11] spectral line compilation was used as input data to obtain the group parameters. The application of this method is especially effective for gases presented in both the jet and the atmosphere ( $\text{H}_2\text{O}$  and  $\text{CO}_2$ ) because it takes into account ‘‘hot lines’’ that arise between high energy levels and that experience only slight absorption in the atmosphere.

In the three-group method the lines in each spectral interval  $\Delta\nu$  are approximated by three groups of lines with the same lower energy levels and the same intensity within each group. A position of each line is random and statistically independent of the lines of both the same and other gases. The temperature dependence of the absorption coefficient stipulated by the lines of one group is approximately the same for all the frequencies within the spectral interval, since it is defined mostly by the energy of the lower level. So, the effective radiation volume  $G$  for the lines of one group does not depend on frequency and only the production of the atmosphere transmittance and jet absorption coefficients has to be averaged. The Curtis–Godson approximation [8, 12] is used to take into account the radiation path non-uniformity. We have

$$\begin{aligned} \overline{k_v \tau} &= \left( \sum_{m,n} k_{mn} \right) \left( \prod_{k,l} \tau_{kl} \right) = \sum_{m,n} \left( \overline{k_{mn} \tau_{mn}} \prod_{\substack{k \neq m \\ l \neq n}} \overline{\tau_{kl}} \right) \\ &= \sum_{m,n} \left( \overline{k_{mn} H_{mn} \tau_{mn}} \prod_{\substack{k \neq m \\ l \neq n}} \overline{\tau_{kl}} \right) = \left( \prod_{k,l} \overline{\tau_{kl}} \right) \sum_{m,n} \overline{k_{mn} H_{mn}} \end{aligned}$$

$$= \overline{\tau} \sum_{m,n} \frac{S_{mn}(T)}{d_{mn}} H_{mn}(T), \tag{24}$$

where the bar designates the frequency averaging,  $m$  is the line group number,  $n$  is the radiating substance number;  $\tau_{mn}$  and  $k_{mn}$  are the atmosphere transmittance and absorption coefficient stipulated by the  $mn$  group of the spectral lines. The quantity  $\overline{\tau}$  is the spectral atmospheric transmittance with respect to a grey source;  $S_{mn}$  is the spectral line intensity, and  $d_{mn}$  is the mean spacing between the lines of the  $mn$  group.

$$\overline{\tau_{mn}} = \exp \left[ -A_{mn} (1 + A_{mn}^2 / B_{mn})^{-1/2} \right], \tag{25}$$

$$A_{mn} = \int_0^L S_{mn}(x) d_{mn}^{-1} dx, \tag{26}$$

$$B_{mn} = 4 \int_0^L S_{mn}(x) \gamma(x) d_{mn}^{-2} dx, \tag{27}$$

$\gamma$  is the Lorenz line half-width. The integrals in eqns (26) and (27) are taken along the atmosphere path with the length  $L$  between the jet and a receiver;  $H_{mn}$  is the frequency correlation between jet radiation and atmospheric absorption stipulated by the  $mn$  group of the spectral lines:

$$H_{mn}(T) = \left( 1 + \frac{2\gamma(T) A_{mn}^3}{d_{mn} B_{mn}^2} \right) \left( 1 + \frac{A_{mn}^2}{B_{mn}} \right)^{-3/2}. \tag{28}$$

In eqn (24) the line intensity  $S_{mn}(T)$  varies directly as the  $n$ -gas concentration and depends on the jet temperature. The function  $H_{mn}(T)$  depends on the jet temperature only by means of the line half-width. Taking into account eqn (24), we can write the spectral radiation intensity of the circular jet as

$$\begin{aligned} \overline{S}(\xi) &= 2R_0^3 X_T \overline{\tau} [B(T_0) - B(T_\infty)] \\ &\times \sum_{m,n} C_{0n} \frac{S_{mn}^{STP}(T_0)}{d_{mn}} \frac{300}{T_0} H_{mn}(T_0) \\ &\times G \left( \xi, F, \frac{a_{mn}}{T_0}, \frac{b}{T_0}, \frac{\Delta T_0}{T_0}, \frac{\Delta C_{0n}}{C_{0n}} \right), \end{aligned} \tag{29}$$

where  $a_{mn}$  is an analog of the constant  $a$  from eqn (17):

$$a_{mn} = T_0^2 \frac{d}{dT_0} \ln \left\{ \frac{S_{mn}^{STP}(T_0) 300}{d_{mn} T_0} \right\}. \tag{30}$$

As  $H_{mn}$  depends only slightly on the temperature, we used in eqn (29) the constant value  $H_{mn}(T_0)$  which is close to the magnitudes of  $H_{mn}$  in the jet region giving main contribution into the value of the integral (15).

Direct computation of the values of  $G$  using eqns (18)–(21) requires the knowledge of the functions  $f(\xi, \eta)$  and  $R(F, \xi)$ . It is more convenient to estimate the values  $g_k$  ( $k = 0, 1$ ) by numerical integration of the expression  $C^k(x, r) \exp[-A/T(x, r)]$  over the jet

Table 1. The values of the effective radiating volume determined numerically

$F$	$\Delta T_0/T_0$	$A/T_0$								
		1	2	4	6	8	10	15	20	25
1	0.2	2.77	2.48	2.02	1.68	1.43	1.25	0.95	0.78	0.67
	0.3	2.58	2.17	1.62	1.27	1.06	0.91	0.70	0.59	0.53
	0.4	2.37	1.88	1.31	1.01	0.84	0.73	0.58	0.51	0.47
	0.45	2.27	1.74	1.19	0.92	0.77	0.67	0.55	0.49	0.45
5	0.2	3.19	2.84	2.30	1.90	1.61	1.40	1.05	0.86	0.74
	0.3	2.96	2.48	1.82	1.43	1.18	1.01	0.77	0.64	0.57
	0.4	2.71	2.13	1.46	1.12	0.93	0.80	0.63	0.55	0.50
	0.45	2.59	1.97	1.32	1.02	0.84	0.74	0.59	0.52	0.47
50	0.2	3.91	3.47	2.78	2.28	1.91	1.63	1.18	0.93	0.78
	0.3	3.62	3.01	2.18	1.67	1.35	1.13	0.82	0.66	0.57
	0.4	3.31	2.58	1.72	1.28	1.02	0.86	0.64	0.54	0.48
	0.45	3.15	2.38	1.54	1.14	0.91	0.78	0.59	0.50	0.45

volume followed by normalization of the result with respect to the expression  $2R_0^3 X_T C_0^k \exp(-A/T_0)$ . The values of  $g_1$  computed by this method at  $\xi = 2$  are presented in Table 1 for three Froude numbers.

The spectral intensity of radiation emitted by a buoyant jet containing only water vapour and carbon dioxide was calculated by two methods. The first (traditional) method [12] includes calculation of the jet concentration and temperature fields followed by numerical integration over the jet surface area of the spectral radiance that passed through the atmosphere. The second method is based on the use of eqn (29) and the effective radiation volume data from Table 1.

The comparison was carried for a vertical jet with the following outlet parameters:  $T_0 = 475$  K,  $D = 2$  m,  $C_0(\text{CO}_2) = C_0(\text{H}_2\text{O}) = 0.04$ . The atmosphere parameters were chosen in the following manner:  $T_\infty = 273$  K,  $C_\infty(\text{CO}_2) = 0.00033$ , atmospheric pressure was 1 atm, humidity was 80%. In the case under consideration we can neglect the content of  $\text{CO}_2$  and  $\text{H}_2\text{O}$  in the atmosphere and put  $G = g_1$ .

The validity limits of the optically thin approximation were given previously [13]. The approach based on eqn (29) may bring a large error in the spectral regions where the optically thin approximation is violated. It can take place in the absorption bands of the main combustion products of the hydrocarbon fuels  $\text{CO}_2$  and  $\text{H}_2\text{O}$  if the distance of viewing is not large enough. As it is seen from Fig. 7, where the jet spectral intensity in the  $4.3 \mu\text{m}$  band of  $\text{CO}_2$  is presented, the result based on eqn (29) differs considerably from the exact one [12] at relatively small distance of 200 m (see Fig. 7(a)). But the "non-volumetric" portion of radiation is absorbed by the atmosphere and the discrepancy between the exact method [12] and the approximation based on eqn (29) becomes smaller as the viewing distance increases. It can be seen from Fig. 7(b) where the results for the distance of 10 km are presented. Similar comparison is shown in Fig. 8 for the spectral range from 2–14  $\mu\text{m}$  at the atmosphere layer of 5 km thick. The discrepancy

between the two calculation techniques does not exceed 20 or 30%. A noticeable difference (up to 100%) is observed only in the narrow spectral interval in the region of the  $\text{CO}_2$   $4.3 \mu\text{m}$  band.

Thus, the method based on eqn (29) reduces the computational expenditures considerably and provides a reasonable accuracy in the prediction of the thermal radiation of buoyant turbulent jets. The method does not require a detailed information about the jet gas dynamics structure and gives a simple relation between the jet radiation intensity and the outlet jet parameters.

## 6. CONCLUSION

An attempt has been made in this paper to establish the thermal radiation similarity of buoyant turbulent jets. The principal condition of the optical similarity is the similarity of the temperature and the concentration fields in the near-nozzle region because the main portion of radiation is generated by the most heated section of the jet. The  $k-\epsilon-T'^2$  turbulent viscosity model was used to study the gas dynamic similarity in the near-nozzle zone. This model adequately describes all the known experimental data concerning heated buoyant turbulent jets. It has been shown that longitudinal ( $X_T$ ) and transverse ( $R_T$ ) scales can be introduced. In general, these scales depend on the initial turbulence level and the Froude number. The excess temperature and concentration are described by an universal function for the wide range of the jet outlet parameters if the dimensionless coordinates  $\xi = x/X_T$  and  $\eta = r/R_T$  are used.

As a result of the gas dynamic similarity it has been found that dimensionless spectral intensity (normalized with respect to the production of spectral radiance at the edge of the nozzle and the nozzle area) is described by the universal function which is the same for a wide class of jets and depends on the exit thermodynamic parameters, radiation frequency and

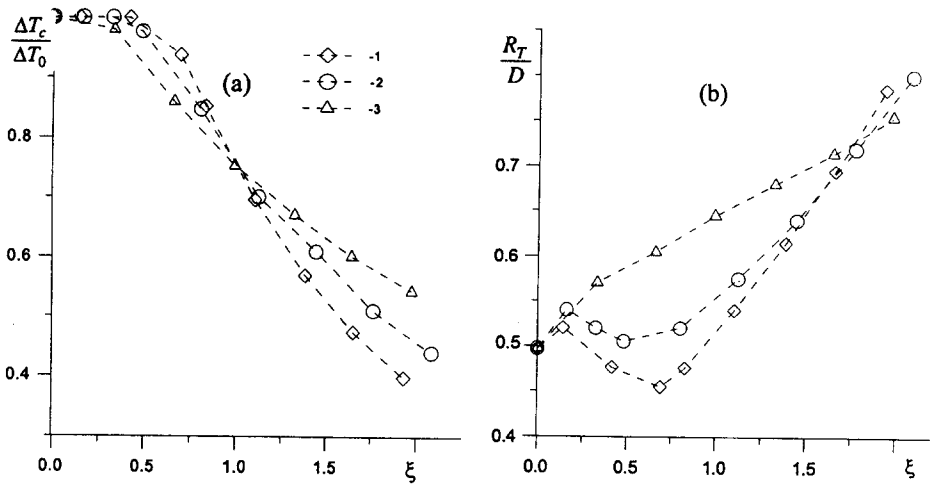


Fig. 6. Dependence of the excess temperature (a) and radial thermal scale (b) on the dimensionless axial coordinate of a buoyant jet ( $F = 5$ ) for various initial levels of turbulence. (Designations are the same as in Fig. 5.)

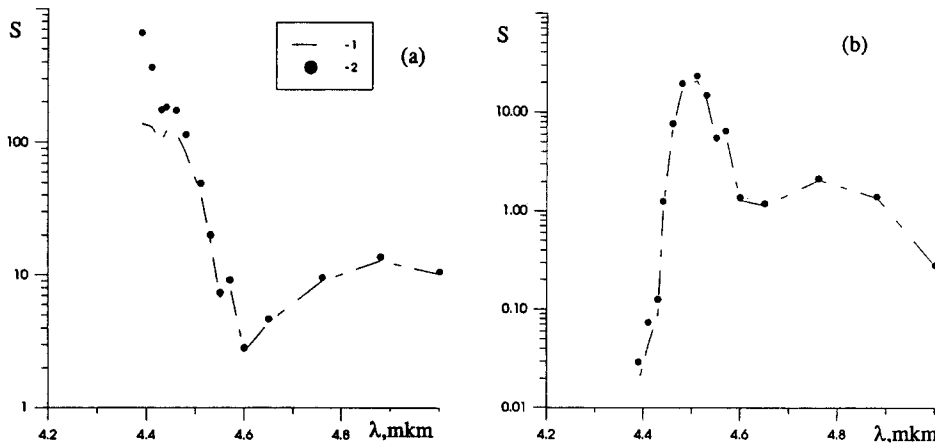


Fig. 7. Spectral distribution of radiation intensity ( $W/\mu\text{m sr}$ ) of the jet near-nozzle section for viewing distances of 200 m (a) and 10 km (b). 1, calculations on the basis of numerical integration over the jet area [11]; 2, calculations with their use of the optical similarity relationships.

on the steepness of the temperature dependence of the absorption coefficient.

The results obtained have been generalized for the radiation of molecular gases in finite spectral intervals containing many spectral lines. The three-group statistical band model was used for this purpose. The relationship between the jet radiation intensity and the outlet and spectroscopic parameters has been found. A simple and effective method for jet radiation prediction

has been developed. The method does not require a detailed information about the jet gas dynamics structure. The method is reduced to the calculation of the spectral radiance at the nozzle edge followed by multiplication by the effective radiative volume. The traditional method includes prior calculation of the gas dynamic structure followed by numerical integration of the radiation transfer equation. The results obtained by two methods are in a good agreement.

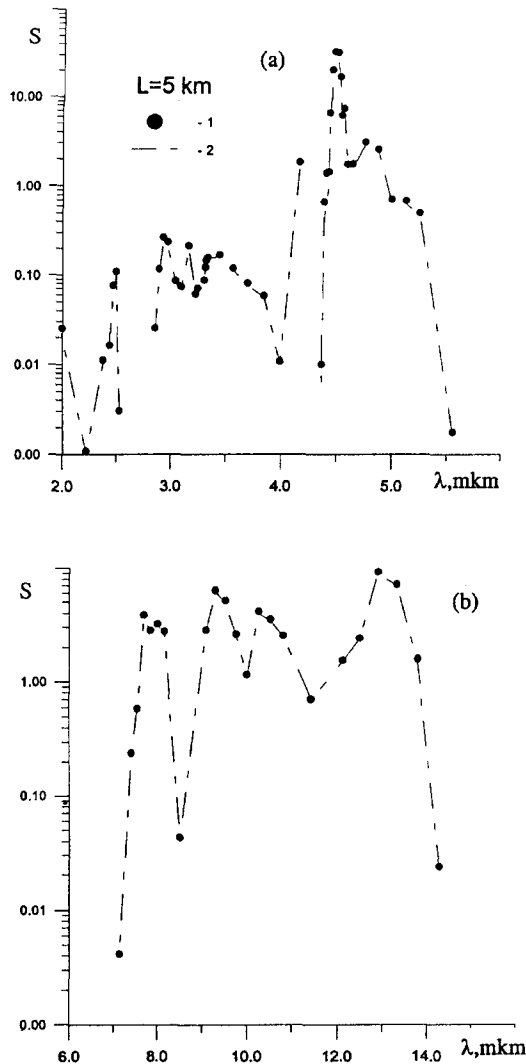


Fig. 8. Spectral distribution radiation intensity ( $W/\mu m \text{ sr}$ ) of a jet near-nozzle section for the viewing distance of 5 km. 1, calculations on the basis of numerical integration over the jet area [11]; 2, calculations with the use of the optical similarity relationships.

*Acknowledgements*—The authors are very thankful to Prof. Yu. V. Khodyko for the helpful discussion of this work. This work was partially supported by the International Science Foundation and the Government of the Republic of Belarus under the grant #F95100.

## REFERENCES

1. Belyayev, Yu. V., Kuzmin, A. N., Zhdanovich, O. B. and Khodyko, Yu. V., Experimental verification of optical similarity of heated molecular jets. *High Temperature*, 1991, **29**, 961–966.
2. Bril, A. I., Kabashnikov, V. P. and Khodyko, Yu. V., The similarity of the radiation properties of heated jets. *High Temperature*, 1991, **29**, 995–1001.
3. Chen, C. J. and Nikitopoulos, C. P., On the near field characteristics of axisymmetric turbulent buoyant jets in a uniform environment. *Int. J. Heat Mass Transfer*, 1979, **22**, 245–255.
4. Chen, C. J. and Chen, C. H., On prediction and unified correlation for decay of vertical buoyant jets. *J. Heat Transfer*, 1978, **101**, 245–255.
5. Abramovich, G. N., *Theory of Turbulent Jets*. Izd. Nauka, Moscow, 1984.
6. Khodyko, Yu. V., Bril, A. I. and Zhdanovich, O. B., Utilization of model passive impurity concentration distribution functions to compute turbulent flow radiation. *J. of Eng. Phys.*, 1989, **57**, 1005–1012.
7. Frost, W. and Moulden, T. H., ed., *Handbook of Turbulence. Volume 1. Fundamentals and Application*. NY, 1977.
8. Goody, R. M., *Atmospheric Radiation*. Oxford University Press, Oxford, 1964.
9. Penner, S. S., *Quantitative Molecular Spectroscopy and Gas Emissivities*. Addison-Wesley, Reading, MA 1959.
10. Khodyko, Yu. V., Kurskov, A. A. and Antiporovich, N. V., The multi-group method for calculating the selective IR radiation transfer in inhomogenous media. *J. of Applied Spectrosc.*, 1986, **44**, 284–288.
11. Rothman, L. S., Gamache, R., Goldman, A. *et al.*, The 1986 edition of the HITRAN database compiled by the Air Force Geophysics Laboratory, *Applied Optics*, 1987, **26**, 4058–4097.
12. Ludwig, C. B., Malcmus, W., Reardon, J. E. and Thompson, J. A. L., *Handbook of Infrared Radiation from Combustion Gases*. Scientific and Technical Information Office, Washington, DC, 1973.
13. Bril, A. I., Kabashnikov, V. P., Kuzmina, N. V. and Khodyko, Yu. V., A method for computing the IR radiation of molecular gas jets in the volumetrical approximation, *J. of Applied Spectrosc.*, 1991, **55**, 934–939.